Mid–callosal plane determination using preferred directions from diffusion tensor images

André L. Costa[a] and Letícia Rittner[a] and Roberto A. Lotufo[a] and Simone Appenzeller[b]

[a]Department of Computer Engineering and Industrial Automation
School of Electrical and Computer Engineering, University of Campinas
400 Albert Einstein st, 13083–852, Campinas, Sao Paulo, Brazil;
[b]School of Medicine, Rheumatology Unit, University of Campinas
Alexander Fleming st, 13083–970, Campinas, Sao Paulo, Brazil

ABSTRACT

The corpus callosum is the major brain structure responsible for inter–hemispheric communication between neurons. Many studies seek to relate corpus callosum attributes to patient characteristics, cerebral diseases and psychological disorders. Most of those studies rely on 2D analysis of the corpus callosum in the mid–sagittal plane. However, it is common to find conflicting results among studies, once many ignore methodological issues and define the mid–sagittal plane based on precary or invalid criteria with respect to the corpus callosum. In this work we propose a novel method to determine the mid–callosal plane using the corpus callosum internal preferred diffusion directions obtained from diffusion tensor images. This plane is analogous to the mid–sagittal plane, but intended to serve exclusively as the corpus callosum reference. Our method elucidates the great potential the directional information of the corpus callosum fibers have to indicate its own referential. Results from experiments with five image pairs from distinct subjects, obtained under the same conditions, demonstrate the method effectiveness to find the corpus callosum symmetric axis relative to the axial plane.

Keywords: Corpus Callosum, Mid–Callosal Plane, DTI, Mid–Sagittal Plane, Registration

1. INTRODUCTION

The *corpus callosum* (CC) is the largest white matter structure found in mammalian brain.[1] It is basically composed by axons that connect neurons from both brain hemispheres. There is a large number of publications in the literature from studies that seek to relate CC attributes to patient characteristics, like sex and age,[2] and to cerebral diseases[3,4] and psychological disorders,[5,6] like Alzheimer, lupus, ADHD, and autism. Most of those studies rely on a 2D analysis of the CC in the *mid–sagittal plane* (MSP). However, as stated by Mitchell et al.,[2] it is common to find disagreements in results from several studies due to a lack of standardization to define the proper MSP. Many simply ignore this methodological issue and define the MSP based on precary or invalid criteria with respect to the CC analysis.[2,7]

Two interesting methods to find the MSP were proposed respectively by Liu et al.[7] and by Mitchell et al..[2] The former is a fully automated procedure to find a plane which maximize the symmetry from the brain and the head in general. The authors claim the method has high robustness even in pathological scenario. The other method define the MSP based on the identification of three brain points, the *anterior commissure* (AC), the *posterior comissure* (PC), and one point from the *interhemispheric fissure* (IF). This is a simple and effective method, but hard to automate, since the automatic methods for identifying the AC and PC points rely on an analysis of the MSP.[8–10] Nevertheless, what these two methods have in common is that the criteria for finding the MSP is not directly related to the CC, which is true for most methods designed to estimate the MSP. The reason these methods rely on data outside the CC to find a plane that will serve as its reference may be related to the CC shape complexity, hard to identify in planes other than the sagittal.

Further author information: (Send correspondence to A.L.Costa)
A.L.Costa: E-mail: alcosta@dca.fee.unicamp.br, Telephone: +55 19 99837 4949

Medical Imaging 2015: Biomedical Applications in Molecular, Structural, and Functional Imaging,
edited by Barjor Gimi, Robert C. Molthen, Proc. of SPIE Vol. 9417, 94172A

Lets consider that the CC has one unique plane which serves as primary reference for the structure, the ideal *mid–callosal plane* (MCP). Then, the expected properties for this ideal MCP are: (i) the plane will cross the exact middle of the corpus callosum, relative to the sagittal plane of the subject coordinate system; (ii) the ideal MCP must be the same for multiple images from the same subject. This means that the CC shape on the ideal MCP will be almost the same for all images, except for noise and distortions introduced in image acquisition, and for variations in the subject physiology due to aging or disease progression/regression; (iii) the ideal MCP should be located in an equivalent region in brains from distinct subjects. Therefore, the CC shape should also be very similar between health subjects, where differences would be mainly due to individual inherent characteristics. These conditions are essential to perform any robust analysis intra and inter–subject in longitudinal and comparative studies involving the CC.

In this work we propose a novel method to find an estimation of the ideal MCP. Instead of looking for landmarks on anatomical images, we seek indicators of such plane from the CC internal fiber arrangements, revealed by *diffusion tensor images* (DTI). Specifically, the proposed method searches for a plane that optimize the symmetry of the CC fiber structure, as described in details in Section 2. Experiments to assess the method accuracy on predicting the ideal MCP are reported in Section 3, along with a discussion about the obtained results. Ultimately, a conclusion and suggestions for future works are given in Section 4.

2. THE PROPOSED METHOD

The proposed method uses DTI to define a MCP according to the CC internal preferred diffusion directions, i. e., the directions of the eigenvectors associated to the largest eigenvalues from the CC tensors. The method main goal is to predict a geometric transformation to make the current MCP* parallel to the ideal MCP. As illustrated in Fig. 1(a), this transformation requires two rotations and one translation: the first rotation is about the $\vec{z}$ axis, determined by θ to make the projection of $\vec{y'}$ axis in the axial reference plane parallel to axis $\vec{y}$. The second rotation is in the coronal plane, about $\vec{y}$ axis by an angle φ so that $\text{proj}_{xz}(\vec{z'})$ is parallel to $\vec{z}$. Finally, a translation on axis $\vec{x}$ is applied. The diagram at Fig. 1(b) introduces an overview of the workflow to find the transformation which aligns both planes, current and ideal MCP.

2.1 Preprocessing

In the preprocessing step, the volume is reoriented to have the axis $\vec{x}$ normal to the sagittal plane, the axis $\vec{y}$ normal to the coronal plane, and the axis $\vec{z}$ normal to the axial plane. The CC *volume of interest* $\text{VOI} \subset \mathbb{N}^3$ is then defined by the bounding box of a 2D CC segmentation on the current MCP expanded 10 mm to the left and another 10 mm to the right in the $\vec{x}$ axis. For the 2D CC segmentation we employed the method proposed by Freitas et al.,[11] which includes the identification of the sagittal slice closest to the *interhemispheric fissure* (IF), taken as the current MCP.

Let $V : \text{VOI} \mapsto \mathbb{R}^3$ be a volume of eigenvectors correspondent to the largest eigenvalues from tensors. These eigenvectors represent the preferred water diffusion directions in the brain, and are the basis for the proposed method as they give the fiber orientations in the CC structure. All vectors $\vec{v} \in V$ should have the same orientation relative to the $\vec{x}$ axis.

2.2 The Axial Rotation Angle

The next step is to define the axial rotation angle θ from directions of the vectors $\vec{v} \in V$. As shown in Fig. 2(a), the eigenvectors reveal a symmetrical arrangement in the CC fibers, and in the highlighted columns it is possible to observe that the directions of the eigenvectors vary gradually along the sequence of voxels. By the analysis of a set of *inclination variation sequences* (IVS), such as those highlighted, we can have a cost value that reflects the fiber's symmetry axis alignment, for a given volume rotation. The plot presented in Fig. 2(d) was generated from the obtained cost values after rotating a sample volume by θ values ranging from -10° to +10° . Finally, a linear function $\overline{J}(\theta)$ is predicted from the sampled cost values, and θ is defined as the one that nullifies $\overline{J}$.

*The current MCP refers to a plane parallel to the sagittal slices of the current volume. The current MCP changes each time a transformation is applied to the current volume.

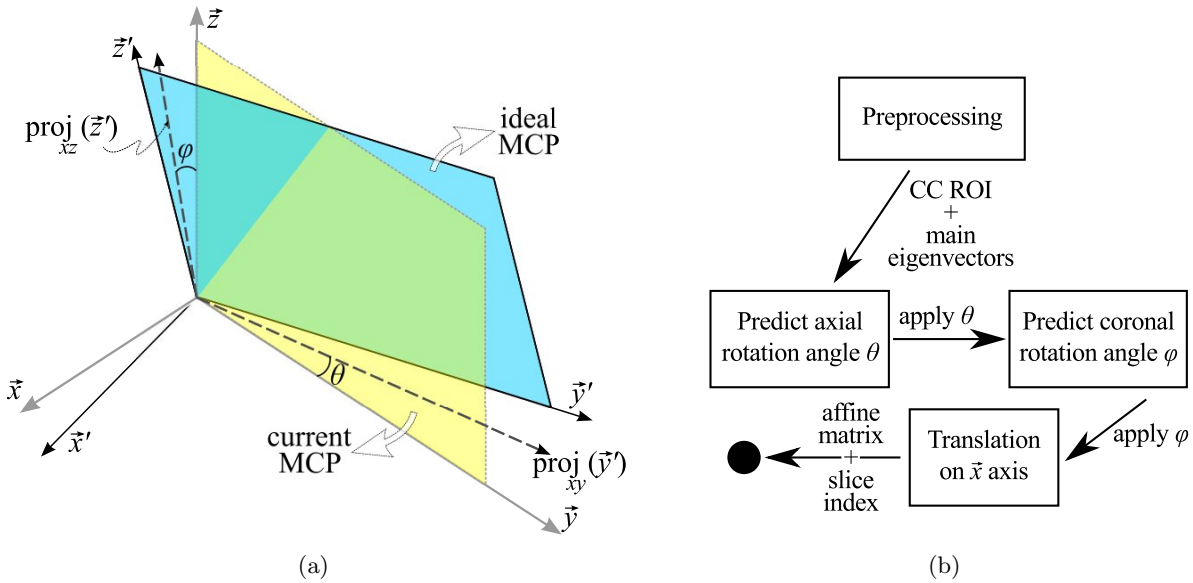

(a) (b)

Figure 1. Method overview. (a) simplified relation between the ideal MCP and the current MCP, regarding rotation angles θ for the axial plane and φ for the coronal plane. (b) workflow overview showing the intermediary procedures (boxes), and the relevant output data (arrows) from each procedure. The final output is an affine transformation matrix and the slice index correspondent to the MCP at the transformed space.

To compute the cost value for a given value of θ we first rotate the original volume accordingly. Then, for each axial projection $\text{proj}_{xy}(\vec{v})$ an inclination angle $i(\text{proj}_{xy}(\vec{v}), \vec{x})$ is calculated relative to $\vec{x}$ axis, generating $I_{axial} : \text{VOI} \mapsto \mathbb{R}$, so that $I_{axial}(x, y, z) = i(\text{proj}_{xy}(\vec{v}), \vec{x})$. Each inclination angle is computed to be in the range $[-\frac{\pi}{2}, \frac{\pi}{2}]$, with $i(\text{proj}_{xy}(\vec{v}), \vec{x}) = 0$ if $\text{proj}_{xy}(\vec{v}) \parallel \vec{x}$. Now, if we take an IVS from I_{axial} along a line with direction normal to the current MCP, we will have an 1D discrete function that describes the arrangement of fibers in that given sector of our VOI. In fact, we can have one of these functions for each coordinate $(y, z) \in \text{VOI}$, in the form $\text{IVS}_{(y,z)} : \mathbb{N} \mapsto \mathbb{R}$, with $\text{IVS}_{(y,z)}(x) = I_{axial}(x, y, z)$, $x \in \text{VOI}$.

To better understand the role of an $\text{IVS}_{(y,z)}$ on θ prediction, lets take a look at Fig. 2. The vector field shown in Fig. 2(a) was generated from the axial projections of eigenvectors $\vec{v} \in V_{sample} : \text{VOI}_{sample} \subset \mathbb{N}^3 \mapsto \mathbb{R}^3$, for an arbitrary axial slice $z = z_a$. It is possible to visualize that fibers from anterior (left) and posterior regions of the CC have opposite symmetrical curved arrangements. Also, notice that each column in the vector field corresponds to the domain of an $\text{IVS}_{(y,z_a)}$, $y \in \text{VOI}_{sample}$. As illustrated in Fig. 2(b), which contains graphical representations for the highlighted $\text{IVS}_{(15,z_a)}$ and $\text{IVS}_{(64,z_a)}$, an $\text{IVS}_{(y,z)}$ can be nearly linear, with positive or negative linear coefficient, according to the curved arrangement of fibers. Now, let $\overline{\text{IVS}}_{(y,z)} : \mathbb{R} \mapsto \mathbb{R}$ be the linear regression from an $\text{IVS}_{(y,z)}$. Then, $\exists x_0 \in \mathbb{R}$ such that $\overline{\text{IVS}}_{(15,z_a)}(x_0) = \overline{\text{IVS}}_{(64,z_a)}(x_0)$, once $\overline{\text{IVS}}_{(15,z_a)}$ is not parallel to $\overline{\text{IVS}}_{(64,z_a)}$. Our hypothesis is that due to the symmetric nature of the fiber arrangements observed in the corpus callosum, in a perfect scenario with the volume aligned in relation to the ideal MCP, $\overline{\text{IVS}}_{(y,z)}(x') = 0$, where x' intercepts the ideal MCP. Therefore, if the volume is aligned to the ideal MCP, then any two $\text{IVS}_{(y_0,z_0)}$ and $\text{IVS}_{(y_1,z_1)}$, not parallel to each other, should cross at angle 0, i. e., $\overline{\text{IVS}}_{(y_0,z_0)}(x') = \overline{\text{IVS}}_{(y_1,z_1)}(x') = 0$. In addition, if the volume not being aligned to the ideal MCP implies $\overline{\text{IVS}}_{(y_0,z_0)}(x'') = \overline{\text{IVS}}_{(y_1,z_0)}(x'') \neq 0$, then it is possible to define a method to find the rotation that will align the current MCP to the ideal MCP on the axial plane such that $\overline{\text{IVS}}_{(y_0,z_0)}(x') = \overline{\text{IVS}}_{(y_1,z_0)}(x') = 0$.

Since real world is not a perfect scenario, a method using only a pair of $\text{IVS}_{(y,z)}$ to predict θ will certainly lack robustness. Despite that, if we look again at Fig. 2(a) we can clearly see that not all the possible IVS belongs to the CC, or exhibit an linear behaviour, i. e., some IVS are not suitable to assess the volume alignment. Therefore, the method was designed to predict θ based on two sets of selected IVS

$$\mathcal{S}_A = \{\text{IVS}_{(y,z)} \,|e(y, z) < t \text{ and } a(\overline{\text{IVS}_{(y,z)}}) >= 0\}, \tag{1}$$

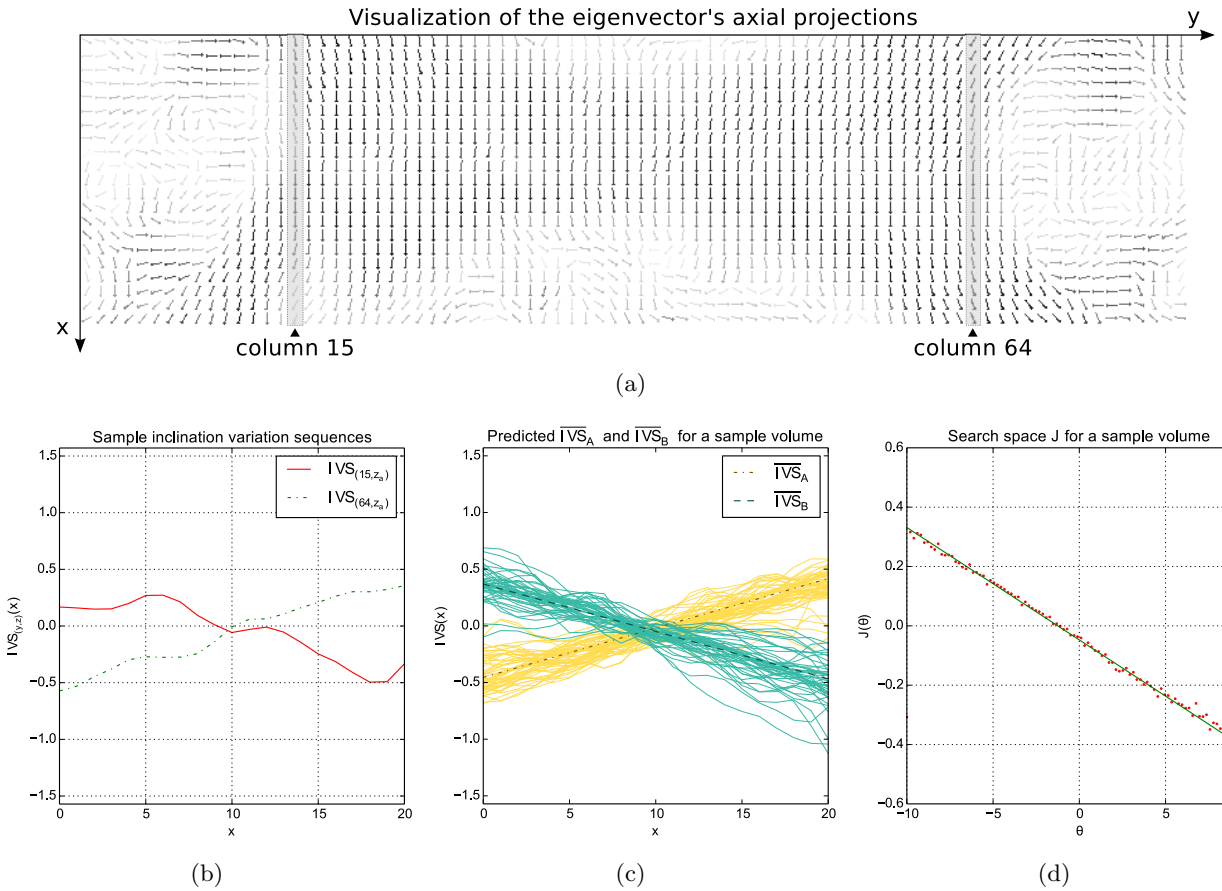

Figure 2. Illustrations from the process to determine θ. (a) vector field generated from the eigenvector projections at the axial plane of a sample volume, showing the symmetrical fiber arrangements that traverse the corpus callosum. (b) graphical representation from the two $\mathrm{IVS}_{(y,z)}$ correspondent to the columns highlighted at Fig. 2(a). (c) plotting of functions $\overline{\mathrm{IVS}}_A$ and $\overline{\mathrm{IVS}}_B$, along with the two respective sets of $\mathrm{IVS}_{(y,z)}$ from where the functions were estimated. The value where the functions intercept each other indicate how well aligned is the volume. (d) $J(\theta)$ samples and the correspondent linear regression $\overline{J}(\theta)$. All angle values for Fig. 2(b–d) are in radians, except for the θ values at Fig. 2(d).

and

$$\mathcal{S}_B = \{\mathrm{IVS}_{(y,z)} \,|e(y,z) < t \text{ and } a(\overline{\mathrm{IVS}_{(y,z)}}) < 0\}, \tag{2}$$

where $e(y,z)$ is the absolute difference from an $\mathrm{IVS}_{(y,z)}$ to its correspondent linear regression $\overline{\mathrm{IVS}}_{(y,z)}$, $a(\overline{\mathrm{IVS}_{(y,z)}})$ is the linear coefficient, and $t = \mu(E) - \sigma(E)$, with $E = \{e(y,z)|(y,z) \in \mathrm{VOI}\}$; μ and σ are respectively the average and standard deviation functions. Observe that only a subset of IVS with good fitness to a linear function are selected. The alignment cost computation follows by performing two robust linear regressions $\overline{\mathrm{IVS}}_A$ and $\overline{\mathrm{IVS}}_B$, respectively over the points stored in sets $\mathcal{S}_A$ and $\mathcal{S}_B$. For the robust regression we employed the RANSAC[12] method in conjunction with an ordinary least square regressor. Graphical representations for two sample $\overline{\mathrm{IVS}}_A$ and $\overline{\mathrm{IVS}}_B$ are shown in Fig. 2(c), together with the IVS in each set. Because these functions were computed from a nearly aligned volume, the two lines crosses in an angle close to 0. Finally, we define the cost function $J : \mathbb{R} \mapsto \mathbb{R}$ as $J(\theta) = \mathrm{IVS}^{\theta}_A(x)$, x is the point where IVS^{θ}_A intercepts IVS^{θ}_B. The cost function J has a well posed linear behaviour, as shown in Fig. 2(d). This, confirms our hypothesis to be true, because there is only one θ for which $\overline{J}(\theta) = 0$, where $\overline{J}$ is a linear regression from J. However, to increase robustness, θ is predicted in two steps. In the first, an intermediary $\overline{J}_i$ is estimated from 10 equally spaced samples taken from the interval $[-10°, 10°]$. Then, θ is defined from a ultimate $\overline{J}$, estimated from another 20 samples also equally spaced in a interval of 2° around the intermediary $\theta_i|\overline{J}_i(\theta_i) = 0$.

2.3 The Coronal Rotation Angle

The first task for φ prediction is to apply the found rotation angle θ to the original volume. From this updated volume, the coronal rotation angle φ is defined in a very similar fashion as the axial rotation angle θ, but now the IVS are computed from the inclination of the eigenvector's coronal projections $\text{proj}_{xz}(V(x,y,z))$, illustrated in Fig. 3(a). Thereby, lets define the volume $I_{coronal} : \text{VOI} \mapsto \mathbb{R}$, so that $I_{coronal}(x,y,z) = i(\text{proj}_{xz}(V(x,y,z)), \vec{x})$ from which the new $\text{IVS}^c_{(y,z)}$ functions will be created. Then, the two robust regressions $\overline{\text{IVS}}^c_A$ and $\overline{\text{IVS}}^c_B$, illustrated in Fig. 3(b), are predicted using the same process as for the axial angle. Even the new cost function $J^c(\varphi)$, depicted in Fig. 3(c), is similar and, consequently, the same approach is employed to predict φ. The major difference for predicting φ lies in the imbalance of the IVS sets used to predict $\overline{\text{IVS}}^c_A$ and $\overline{\text{IVS}}^c_B$, as depicted in Fig. 3(b).

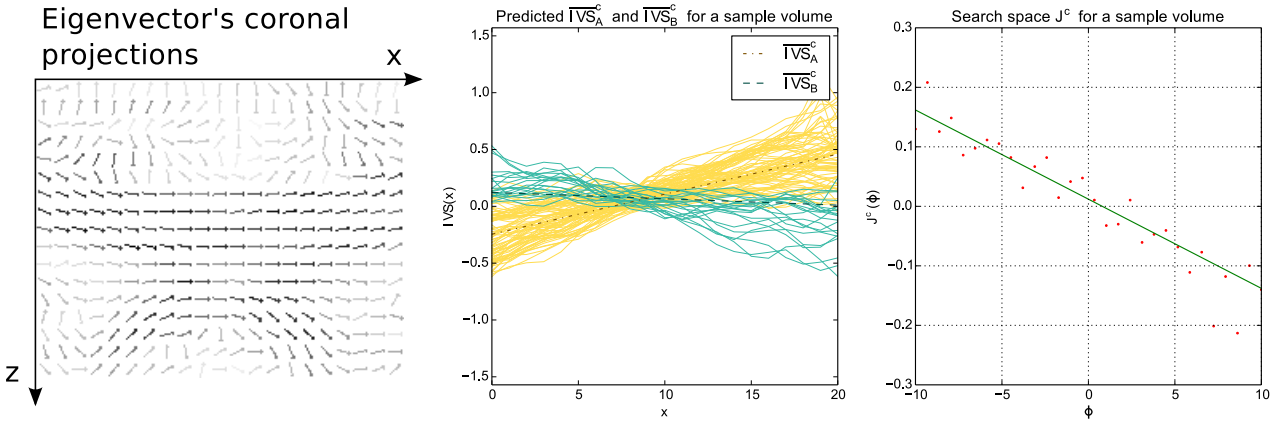

(a) (b) (c)

Figure 3. Illustrations from the process to determine φ. (a) vector field generated from the eigenvector projections at the coronal plane. (b) graphical representation from functions $\overline{\text{IVS}}^c_A$ and $\overline{\text{IVS}}^c_B$. (c) $J^c(\varphi)$ samples and the correspondent linear regression $\overline{J}^c(\varphi)$.

2.4 The Translation

The current MCP for the volume rotated by θ and φ is now parallel to the final predicted MCP, once the rotations were already solved. The last task is to determine the translation that will make the current MCP coincide with the estimated ideal MCP. Thus, the translation in axis $\vec{x}$, normal to the sagittal plane, is determined by the position where $\overline{\text{IVS}_A}$ intercepts $\overline{\text{IVS}_B}$, after the volume is rotated by the found θ and φ. The final output are an *affine matrix* that place the predicted MCP parallel to the volume sagittal slices, and the correspondent *slice index* in the transformed volume, determined by the found translation.

3. EXPERIMENTS

The experiments were designed to validate the effectiveness of the proposed method and developed algorithm. Therefore, the test results provide information to determine the algorithm output correctness and help to analyze if the estimated MCP is an approximation of the ideal MCP, according to its expected properties described in Section 1. The first question we are interested to answer is, will the predicted parameters be the same each time the algorithm is executed? Since the implementation rely on random choices at some stages, like the robust regressions, it may lead to different results for distinct executions using the same input. The answer to that question does not depend on the method effectiveness on finding the ideal MCP, once we are just interested on the output consistency. Therefore, the first experiment, namely, repeatability test, is for testing the method accuracy on predicting θ, φ and the translation on axis $\vec{x}$ for the same volume across multiple runs. Another question we can answer by performing experiments is, will the predicted plane in one image from a subject correspond to the predicted plane in another image from the same subject? A positive answer to this question means that the method is indeed targeting a specific area in the subject brain, instead of a random one. Thus, the

second experiment is conducted on image pairs acquired from the same subject, in order to test the intra–subject correspondence of the predicted plane. Although the results from this second experiment can directly confirm if the estimated MCP has the second property expected for the ideal MCP, they are not enough to confirm the third property. The first and third properties will be analyzed in Section 3.3 through the visualization of the CC in the estimated MCP.

3.1 Data Acquisition and Subjects

The images used in the experiments were acquired from five health subjects in a Philips Achieva magnetic resonance scanner with field strength 3T. Four subjects were female with age ranging from 23 to 26 years old. The fifth subject was a male with age 58. All subjects were scanned twice under the same protocol. Two acquisition pairs were made in 2010, each pair 6 months away, and the other three pairs were acquired on the same day in 2014. The volumes were composed by 2D axial slices, each slice with spacial resolution of 1mm x 1mm, with spacing between slices of 2mm. The diffusion weighted images were scanned from 33 directions, using spin echo DwiSE sequence, and b-value 1000. The final DTI were generated using the software FSL version 5.0.[13]

The acquisition protocol used in this work includes an alignment of the field of view by the scanner operator relative to the brain structures of the subject. The main goal is to align the subject sagittal plane to the volume grid. The operator does the alignment based on an anatomical pre–image of the subject brain, relying mainly in the IF and major brain structures, including the CC.

3.2 Test Procedures and Results

The proposed method and the test routines were implemented using the programming language Python,[14] with Numpy, Scikits–Learn,[15] and NiBabel packages. The code was not optimized for performance, once it is still a prototype designed to test the method validity. The execution time to align one of the tested volumes was about 4 minutes in a machine with processor Intel of 3.4 GHz, and Linux operational system. About 1.5 G Bytes of memory was allocated by the application process.

3.2.1 Repeatability Test

This experiment procedure is intended to verify the repeatability of the predicted parameters θ, φ, and the translation on axis $\vec{x}$. Thus, the output parameters from 10 executions for each image were analyzed to verify the output consistency. The variability of the output values was measured by the standard deviation, shown in Table 1 along with the mean values for each image and output parameters.

Table 1. Predicted parameters for the five tested volume pairs.

	Pair	Predicted θ	Predicted φ	Slice index
Subject 1	1	-1.21° σ0.04	1.18° σ0.19	124 σ0.25
	2	-1.24° σ0.03	6.27° σ0.18	125 σ0.24
Subject 2	1	-2.08° σ0.10	5.34° σ0.23	125 σ0.34
	2	1.89° σ0.10	0.39° σ0.26	132 σ0.43
Subject 3	1	-0.66° σ0.06	-0.08° σ0.24	127 σ0.38
	2	0.43° σ0.06	-1.97° σ0.25	131 σ0.15
Subject 4	1	-1.21° σ0.02	3.07° σ0.17	125 σ0.21
	2	-2.18° σ0.04	2.86° σ0.25	123 σ0.23
Subject 5	1	-0.44° σ0.06	-1.78° σ0.26	128 σ0.24
	2	0.48° σ0.06	-3.96° σ0.18	131 σ0.12

According to the results from this test, the prediction of θ is very consistent, with average standard deviation lesser than a tenth of one degree. However, the prediction of φ is less robust, with standard deviation around a quarter of one degree. A great difference in relation to θ. For the last parameter the average standard deviation was around $0.3mm$. A very small variation, meaning that almost always the same slice in the transfomed volume from any run will be indicated by the method as the MCP.

3.2.2 Intra–Subject Correspondence Test

The main goal for this experiment was to assess if the predicted planes on a pair of images from the same subject are correspondent, i. e., if the distance between them is small. To achieve that we first generated a *mean diffusivity* † (MD) volume from each image pair. Then, each MD volume in the pair was transformed using the respective predicted parameters. The transformation was performed so that the two predicted planes match if the volumes are overlaid. Therefore, if the found planes correspond to exactly the same physical area in the subject's brain, then a registration procedure should not rotate the target volume in the axial and coronal planes, nor translate along the $\vec{x}$ axis. Thus, we perform a rigid body registration procedure using one of the transformed MD volumes as reference and the other as target, and extract the mismatch parameters θ_{reg}, φ_{reg}, and $t^{\vec{x}}_{reg}$ from the resulting registration matrix. The parameters are related respectively to the rotations in the axial and coronal plane, and to the translation. These mismatch parameters were used to analyze the displacement of the predicted planes, and are being presented in Table 2. The registration was performed using the software FSL/Flirt, version 5.0. The original images were also registered to provide a comparison basis relative to human manual alignment by anatomical structures, since the acquisition protocol includes such procedure.

Table 2. Mismatch parameters estimated by performing the registration of the original volume pairs and the aligned volume pairs.

	Pairs	Mismatch θ_{reg}	Mismatch φ_{reg}	Mismatch $t^{\vec{x}}_{reg}$
Subject 1	Original	0.58°	1.80°	$2.11mm$
	Aligned	0.37° σ0.05	3.56° σ0.24	$1.18mm$ σ0.34
Subject 2	Original	3.53°	1.74°	$3.53mm$
	Aligned	0.37° σ0.21	3.36° σ0.26	$2.57mm$ σ0.53
Subject 3	Original	1.66°	0.98°	$4.81mm$
	Aligned	0.56° σ0.09	0.96° σ0.22	$0.99mm$ σ0.44
Subject 4	Original	0.70°	0.59°	$2.27mm$
	Aligned	0.31° σ0.05	0.39° σ0.21	$0.40mm$ σ0.29
Subject 5	Original	0.66°	0.15°	$2.21mm$
	Aligned	0.23° σ0.05	2.04° σ0.32	$2.14mm$ σ0.34

The obtained results show only a small mismatch around half degree between the predicted planes, in regards to rotation in the axial plane. Also, the mismatch for θ_{reg} was considerably smaller than for the original volume alignment. Notwithstanding, the mismatch in coronal rotation was much greater, reaching more than three degrees for two subjects. For three image pairs the mismatch for φ_{reg} was lesser for the original alignment. The translation mismatch was about $2mm$, and it seems to have high correlation with φ_{reg}.

3.3 Discussion

Considering the good match in the axial plane, and the values predicted for θ, it is clear that the method not only targets a specific brain location, but also a different one from that defined through manual alignment. However, to confirm that the predicted plane is an approximation of the ideal MCP we need to check if their properties match. From the CC visualizations relative to the predicted planes, shown in Fig. 4, we can observe that the shape of the CC is very similar intra and inter–subject, except for individual underlying differences. Further, in all images the CC anterior tip and the fornix are present. Those structures appear in a limited region at the middle of the CC. Therefore, we can confirm that all predicted planes has similar location across subjects, and this location is at the middle of the CC. These findings corroborates that indeed the proposed method is able to estimate the ideal MCP.

†Mean diffusivity is a scalar measure correspondent to the average of the three eigenvalues obtained from the diffusion tensor.[11]

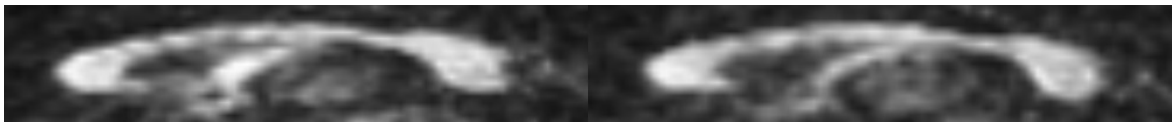

(a) Image pair from subject 1

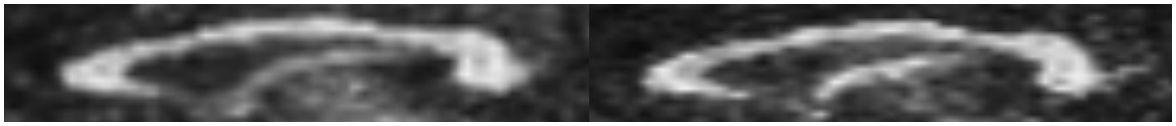

(b) Image pair from subject 2

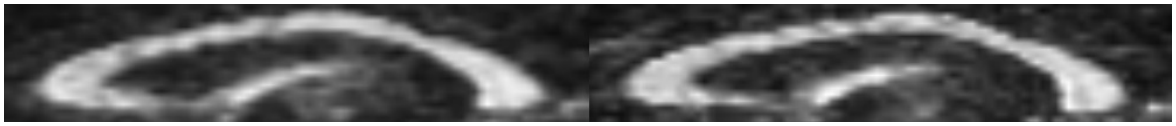

(c) Image pair from subject 3

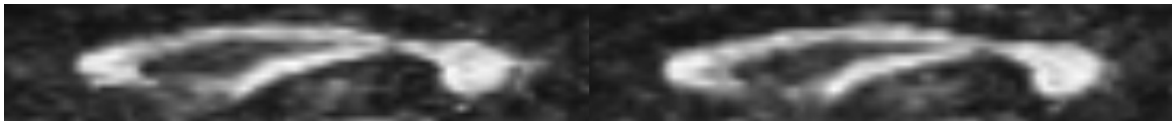

(d) Image pair from subject 4

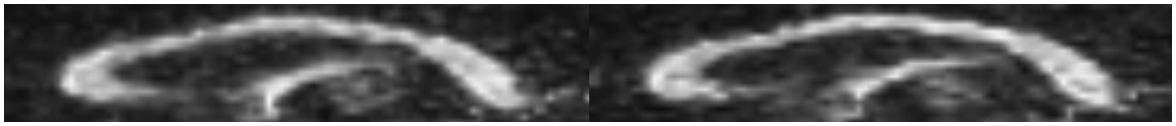

(e) Image pair from subject 5

Figure 4. Visualization of the MCP predicted for each tested image.

Although the results showed that the method was able to estimate the ideal MCP, they also made evident that the method has flaws. The poor prediction of φ is a major one, and can be related to the nearest neighbor interpolation used in the implementation. That would explain the step pattern showed by the cost function $\overline{J}^{c}(\varphi)$, as can be observed in Fig. 3(c). However, only further investigation can reveal the real causes for the φ prediction issue, including its relationship to the plane translation estimation.

The method also has limitations. Once it relies on the symmetrical information of the CC fibers, for subjects that for some reason have asymmetrical arrangement of fibers the method may lead unexpected results. Another limitation is related to the IVS ability to describe the symmetry of fiber arrangements, that may be compromised if the volume is originally too much rotated. However, this last limitation is relatively easy to remove through a slight change in the method.

4. CONCLUSION

In this work we have introduced a novel method to determine the corpus callosum medial plane relative to the subject sagittal plane, so–called mid–callosal plane. The method uses the fiber orientation information to estimate the ideal MSP through the prediction of two rotations, θ and φ, and one translation. The results revealed that the method performs well to predict θ, but has less effectiveness and accuracy in the prediction of φ. Although the method need improvements, it was valid and useful to elucidate the great potential fiber directional information has for the corpus callosum analysis, including determining its own reference. This was the major contribution from this work.

Besides the further investigation needed to improve the method, future studies include analysis of how the variation in the ideal MCP prediction affects different CC characterization techniques, like shape analysis and micro–structural condition assessment using DTI. The results from this study would be useful to determine how accurate the ideal MCP estimation need to be. Another study is to compare the proposed method to other approaches usually employed to determine a reference sagittal plane for the CC analysis.

ACKNOWLEDGMENTS

This work was supported by FAPESP – Fundação de Amparo à Pesquisa do Estado de São Paulo (Foundation for Research Support of the State of Sao Paulo) – grant nº 2012/23059-8.

REFERENCES

[1] Aboitiz, F. and Montiel, J., "One hundred million years of interhemispheric communication: the history of the corpus callosum," *Brazilian Journal of Medical and Biological Research* **36**(4), 409–420 (2003).

[2] Mitchell, T. N., Free, S. L., Merschhemke, M., Lemieux, L., Sisodiya, S. M., and Shorvon, S. D., "Reliable callosal measurement: population normative data confirm sex-related differences," *American Journal of Neuroradiology* **24**(3), 410–418 (2003).

[3] Appenzeller, S., Rondina, J. M., Li, L. M., Costallat, L. T. L., and Cendes, F., "Cerebral and corpus callosum atrophy in systemic lupus erythematosus," *Arthritis & Rheumatism* **52**, 2783–2789 (Sept. 2005).

[4] Di Paola, M., Spalletta, G., and Caltagirone, C., "In vivo structural neuroanatomy of corpus callosum in alzheimer's disease and mild cognitive impairment using different MRI techniques: a review," *Journal of Alzheimer's disease* **20**(1), 67–95 (2010).

[5] Paul, L. K., "Developmental malformation of the corpus callosum: a review of typical callosal development and examples of developmental disorders with callosal involvement," *Journal of neurodevelopmental disorders* **3**(1), 3–27 (2011).

[6] Gozzi, M., Nielson, D. M., Lenroot, R. K., Ostuni, J. L., Luckenbaugh, D. A., Thurm, A. E., Giedd, J. N., and Swedo, S. E., "A magnetization transfer imaging study of corpus callosum myelination in young children with autism," *Biological Psychiatry* **72**, 215–220 (Aug. 2012).

[7] Liu, Y., Collins, R. T., and Rothfus, W. E., "Robust midsagittal plane extraction from normal and pathological 3-d neuroradiology images," *Medical Imaging, IEEE Transactions on* **20**(3), 175–192 (2001).

[8] Verard, L., Allain, P., Travere, J. M., Baron, J. C., and Bloyet, D., "Fully automatic identification of AC and PC landmarks on brain MRI using scene analysis," *Medical Imaging, IEEE Transactions on* **16**(5), 610–616 (1997).

[9] Bhanu Prakash, K., Hu, Q., Aziz, A., and Nowinski, W. L., "Rapid and automatic localization of the anterior and posterior commissure point landmarks in MR volumetric neuroimages1," *Academic Radiology* **13**, 36–54 (Jan. 2006).

[10] Zhang, G., Fu, Y., Wang, S., and Gao, W., "Automatic localization of AC and PC landmarks in t2-weighted MR volumetric neuroimages," in [*Information and Automation (ICIA), 2010 IEEE International Conference on*], 1830–1834, IEEE (2010).

[11] Freitas, P., Rittner, L., Appenzeller, S., and Lotufo, R., "Watershed-based segmentation of the midsagittal section of the corpus callosum in diffusion MRI," in [*Graphics, Patterns and Images (Sibgrapi), 2011 24th SIBGRAPI Conference on*], 274–280 (2011).

[12] Chum, O. and Matas, J., "Optimal randomized RANSAC," *IEEE Transactions on Pattern Analysis and Machine Intelligence* **30**, 1472–1482 (aug 2008).

[13] Jenkinson, M., Beckmann, C. F., Behrens, T. E., Woolrich, M. W., and Smith, S. M., "FSL," *NeuroImage* **62**, 782–790 (Aug. 2012).

[14] Millman, K. J. and Aivazis, M., "Python for scientists and engineers," *Computing in Science & Engineering* **13**(2), 9–12 (2011).

[15] Pedregosa, F., Varoquaux, G., Gramfort, A., Michel, V., Thirion, B., Grisel, O., Blondel, M., Prettenhofer, P., Weiss, R., Dubourg, V., and others, "Scikit-learn: Machine learning in python," *The Journal of Machine Learning Research* **12**, 2825–2830 (2011).